

## Research Article



## OPEN ACCESS

Received: Jan 24, 2020

Revised: Jul 22, 2020

Accepted: Aug 7, 2020

Talabani RM, Garib BT, Masaeli R,  
Zandsalimi K, Ketabat F

### \*Correspondence to

**Ranjdar Mahmood Talabani, BDS, MSc**

Lecturer, Department of Conservative  
Dentistry, University of Sulaimani,  
Sulaymaniyah - Dream Land B-25,  
Sulaymaniyah 46001, Kurdistan Region, Iraq.  
E-mail: ranjdar.osman@univsul.edu.iq

Copyright © 2021. The Korean Academy of  
Conservative Dentistry

This is an Open Access article distributed  
under the terms of the Creative Commons  
Attribution Non-Commercial License ([https://  
creativecommons.org/licenses/by-nc/4.0/](https://creativecommons.org/licenses/by-nc/4.0/))  
which permits unrestricted non-commercial  
use, distribution, and reproduction in any  
medium, provided the original work is properly  
cited.

### Conflict of Interest

No potential conflict of interest relevant to this  
article was reported.

### Author Contributions

Conceptualization: Talabani RM, Garib BT,  
Masaeli R. Data curation: Talabani RM. Formal  
analysis: Talabani RM. Investigation: Talabani  
RM, Zandsalimi K, Ketabat F. Methodology:  
Garib BT, Masaeli RM. Project administration:  
Talabani RM. Software: Ketabat F. Supervision:  
Garib BT, Masaeli R. Validation: Zandsalimi  
K. Visualization: Garib BT. Writing - original  
draft: Talabani RM. Writing - review & editing:  
Garib BT.

# Biom mineralization of three calcium silicate-based cements after implantation in rat subcutaneous tissue

Ranjdar Mahmood Talabani ,<sup>1\*</sup> Balkees Taha Garib ,<sup>2</sup> Reza Masaeli ,<sup>3</sup>  
Kavosh Zandsalimi ,<sup>4</sup> Farinaz Ketabat ,<sup>5</sup>

<sup>1</sup>Department of Conservative Dentistry, University of Sulaimani, Sulaimani, Iraq

<sup>2</sup>Department of Oral Diagnosis, University of Sulaimani, Sulaimani, Iraq

<sup>3</sup>Department of Dental Biomaterial, Tehran University of Medical Sciences, Tehran, Iran

<sup>4</sup>Department of Life Sciences Engineering, Faculty of New Sciences and Technologies, University of Tehran, Tehran, Iran

<sup>5</sup>Division of Biomedical Engineering, University of Saskatchewan, Saskatoon, Canada

## ABSTRACT

**Objectives:** The aim of this study was to evaluate the dystrophic mineralization deposits from 3 calcium silicate-based cements (Micro-Mega mineral trioxide aggregate [MM-MTA], Biodentine [BD], and EndoSequence Root Repair Material [ESRRM] putty) over time after subcutaneous implantation into rats.

**Materials and Methods:** Forty-five silicon tubes containing the tested materials and 15 empty tubes (serving as a control group) were subcutaneously implanted into the backs of 15 Wistar rats. At 1, 4, and 8 weeks after implantation, the animals were euthanized ( $n = 5$  animals/group), and the silicon tubes were removed with the surrounding tissues. Histopathological tissue sections were stained with von Kossa stain to assess mineralization. Scanning electron microscopy and energy-dispersive X-ray spectroscopy (SEM/EDX) were also used to assess the chemical components of the surface precipitates deposited on the implant and the pattern of calcium and phosphorus distribution at the material-tissue interface. The calcium-to-phosphorus ratios were compared using the non-parametric Kruskal-Wallis test at a significance level of 5%.

**Results:** The von Kossa staining showed that both BD and ESRRM putty induced mineralization starting at week 1; this mineralization increased further until the end of the study. In contrast, MM-MTA induced dystrophic calcification later, from 4 weeks onward. SEM/EDX showed no statistically significant differences in the calcium- and phosphorus-rich areas among the 3 materials at any time point ( $p > 0.05$ ).






**Conclusions:** After subcutaneous implantation, biom mineralization of the 3-calcium silicate-based cements started early and increased over time, and all 3 tested cements generated calcium- and phosphorus-containing surface precipitates.

**Keywords:** Biodentine; Biom mineralization; EndoSequence

## INTRODUCTION

Calcium silicate-based cements are biocompatible ceramic compounds. They are neither harmful nor shrinkable and largely remain in a fixed chemical state within biological

## ORCID iDs

Ranjdar Mahmood Talabani   
<https://orcid.org/0000-0002-9833-1013>  
Balkees Taha Garib   
<https://orcid.org/0000-0003-3607-6907>  
Reza Masaeli   
<https://orcid.org/0000-0002-3003-889X>  
Kavosh Zandsalimi   
<https://orcid.org/0000-0002-8877-0565>  
Farinaz Ketabat   
<https://orcid.org/0000-0001-7357-8100>

media [1]. In the 1990s, calcium silicate-based materials were introduced to endodontics as retrograde filling materials [2]. These new calcium silicate cements were composed of tricalcium and dicalcium silicates, calcium phosphates, and calcium hydroxide, as well as zirconium oxide as a radiopacifier [3].

The excellent biocompatibility of these cements is attributed to their analogous relationship with biological hydroxyapatite. During the hydration process, bioceramics generate various material compounds (such as hydroxyapatites) that can trigger a regenerative response in the human body [4].

Calcium silicate bioactive cements upregulate the differentiation of osteoblasts, fibroblasts, cementoblasts, odontoblasts, and many stem cells. When inserted in biological liquid media, they can induce the chemical formation of a calcium phosphate/apatite coating. Their capacity to enhance calcium phosphate deposits is the basis of their use for dentin remineralization and tissue regeneration [5]. *In vitro* studies by Gandolfi *et al.* [6], *in vivo* animal tests by Reyes-Carmona *et al.* [7], and clinical studies [8] have postulated that calcium phosphate deposits could nucleate apatite and promote remineralization to trigger the formation of new mineralized tissues.

Micro-Mega mineral trioxide aggregate (MM-MTA; Micro-Mega SA, Besançon, France) is pre-dosed and supplied in a capsule of tricalcium silicate-based cement. Its newer formulations were designed to minimize the disadvantages of original MTA products, with improved setting and handling. Their composition includes calcium carbonate, which not only decreases the setting time [9] but also is osteoconductive, osteoinductive, and biocompatible. The biological integration of MM-MTA is due to calcium ions, which form hydroxyapatite upon contact with phosphate ions in the body [10].

Biodentine (BD; Septodont, Saint Maur des Fosses, France) was developed as a novel tricalcium silicate-based cement in 2010 [11] that can also serve as a dentin substitute [12]. In addition to its superiority to MTA in terms of manipulation, compatibility, and hardening, it releases significantly more calcium ions with deeper integration into human root canal dentin than MTA [13]. Along with calcium and silicon, the intertubular diffusion of carbonate into the dentin leads to the establishment of a mineral infiltration zone [14].

EndoSequence Root Repair Material putty (ESRRM putty) is another premixed, ready-to-use calcium silicate-based cement. It is manufactured by Brasseler USA (Savannah, GA, USA) for use as an alternative to MTA. Favorable characteristics of ESRRM putty include a shorter setting time and superior handling features [15]. This putty possesses better color stability and handling while exhibiting physiochemical properties comparable to MTA. The essential characteristic is that this material can release calcium and phosphate ions, which are necessary for hydroxyapatite deposition [16].

A number of available *in vivo* laboratory studies have been conducted to assess the bioactivity and biom mineralization capacities of various calcium silicate-based materials. The biom mineralization of MM-MTA and ESRRM putty has not been studied in a rat tissue model, and few studies have assessed the capacity of BD to form an area that stains positive with von Kossa stain, which is suggestive of mineralization, after implantation in an animal model [17,18]. Thus, the aim of the present study was to assess and compare the timing and capacity of calcification associated with MM-MTA, BD, and ESRRM putty using von Kossa

stain. Additionally, this study analyzed the scattering of calcium and phosphorus at the material-tissue interface via scanning electron microscopy (SEM) and energy-dispersive X-ray spectroscopy (EDX) after subcutaneous implantation in rat tissue.

## MATERIALS AND METHODS

The principles of laboratory animal care were applied in this study (National Institutes of Health publication 85–23, 1985). The current study also adhered to national regulations on animal care as approved by the Ethical Committee for Animal Research of University of Sulaimani (No. 9; 6/2/2017). In this study, 15 male Wistar albino rats aged 4–5 months and weighing 250–350 g were used. The animals were bred at controlled room temperature and were provided with water and food ad libitum. Animal care was based on guidance from the Farabi Comprehensive Center of Excellence in Ophthalmology at Tehran University of Medical Sciences. Three commercially available calcium silicate-based cement materials were used (**Table 1**): BD (Septodont), ESRRM putty (Brasseler USA), and MM-MTA capsules (MicroMega).

### Implantation in subcutaneous tissue

In this study, 60 sterile silicon tubes (length, 7 mm; inner diameter, 2 mm; outer diameter, 4 mm; both ends open) were used, 45 of which were filled with the 3 tested cements (15 tubes for each cement), while the remaining 15 tubes were used as negative controls without the insertion of any materials. Thus, each rat received 3 tested materials and 1 empty tube. MM-MTA (MicroMega) was formulated in a pre-dosed capsule and inserted into the tubes according to the manufacturer's guidelines. BD (Septodont) was prepared according to the manufacturer's instructions and condensed into the tubes with an amalgam carrier (Zogear, Shanghai, China) using a small ash condenser (Zogear). ESRRM putty (Brasseler USA) is available as premixed tubes and was ready for direct insertion into the silicon tubes.

After intramuscular injection of 2% xylazine (20 mg/kg; Alfasan, Woerden, the Netherlands) and 10% ketamine (100 mg/kg; Alfasan), the backs of the animals were shaved, sterilization was performed with a 5% iodine solution, and a 2.0-cm incision was made in a head-to-tail orientation with a #15 Bard-Parker blade (Aspen Surgical, Caledonia, MI, USA), creating 2 pockets on each side of the incision. Three silicon tubes, each containing 1 of the 3 tested cements, and an empty tube, serving as the negative control, were implanted in each animal in opposite directions (ESRRM putty, lower right; BD, lower left; MM-MTA, upper right; empty tube, upper left). The skin was closed with a 4-0 silk suture (Lenosilk, Istanbul, Turkey).

At 1, 4, and 8 weeks after implantation, the animals were humanely killed using carbon dioxide. The silicon tubes were removed with the surrounding tissues and fixed in 10% buffered formalin at pH 7.0. The specimens were processed for paraffin embedding, and

**Table 1.** Tested cements

Cements	Manufacturer	Composition	Lot No.
MM-MTA	Micro-Mega SA, Besançon, France	Powder: tricalcium silicate, dicalcium silicate, tricalcium aluminate, bismuth oxide, calcium sulfate dehydrate, and magnesium oxide Liquid: calcium carbonate	71708614
ESRRM putty	Brasseler USA, Savannah, GA, USA	Powder: tricalcium silicate, dicalcium silicate, calcium phosphate monobasic, calcium hydroxide, colloidal silica, water-free thickening agent	B19585
BD	Septodont, Saint Maur des Fosses, France	Powder: tricalcium silicate, dicalcium silicate, calcium carbonate, iron oxide, and zirconium oxide Liquid: water with calcium chloride and soluble polymer (polycarboxylate)	5024200U0

MM-MTA, Micro-Mega mineral trioxide aggregate; ESRRM, EndoSequence Root Repair Material; BD, Biodentine.

5- $\mu$ m tissue sections were cut and stained using the von Kossa technique [17] for histological visualization of calcium deposits (mineralization). Mass deposits appeared black, while dispersed deposits appeared gray [18,19].

### SEM/EDX elemental analyses of the material surface/interface

The tubes and the surrounding tissue ( $n = 4$  in each group) were dehydrated using a graded series of ethanol solutions. After drying, the specimens were embedded in epoxy resin (EPON 812; Taab, Aldermaston, UK). Then, sectioning was performed using an ultra-microtome with a diamond knife. Four sections were prepared for each sample. The sections were mounted on glass slides followed by sputter-coating with a thin gold layer to prevent charging during the SEM investigations. The chemical bulk composition of the material interface and the morphological properties of the root repair cements after mineral deposition were analyzed using a field emission scanning electron microscope (Hitachi-S4160; Hitachi, Tokyo, Japan) at an accelerating voltage of 20 kV with an EDX detector (EDAX, Mahwah, NJ, USA).

### Statistical analysis

Statistical analyses were applied using SPSS version 22 software (IBM Corp., Armonk, NY, USA). Comparisons of the concentrations of the calcium- and phosphorus-rich areas produced by each material were analyzed. The level of significance was set at 0.05. The data were analyzed with the non-parametric Kruskal-Wallis test to enable comparisons between the means of the tested cements at the same time points.

## RESULTS

### Histological analysis of biom mineralization

Tissue sections from the control group did not show any black deposition at the openings at the ends of the inserted empty tubes during the 3 studied periods (**Figure 1A, 1B, and 1C**). The subcutaneous tissue at the openings of the tubes loaded with MM-MTA did not show any deposits at week 1 (**Figure 1D**); however, black positive staining was observed starting at week 4 (**Figure 1E**), and this staining continued to increase until the end of the experiment (**Figure 1F**). In contrast, BD-containing tubes showed grayish dispersed deposits at week 1 (**Figure 1G**) and black dystrophic calcification at weeks 4 and 8 (**Figure 1H and 1I**). Finally, ESRRM putty exhibited positive black staining at all time periods (**Figure 1J, 1K, and 1L**).

### SEM/EDX results

Analysis of SEM and EDX images showed representative images of the chemical composition of connective tissue in contact with the opening surface of the silicon tubes containing the 3 tested materials (MM-MTA, BD, and ESRRM putty) at the 3 time points (weeks 1, 4, and 8) (**Figures 2, 3, and 4**).

SEM examination of the microstructure formed around the inserted silicone tubes filled with MM-MTA, BD, and ESRRM putty showed apatite crystals, mineralization, and formation of a tag-like structure with lateral branches starting at week 1. As the implantation period continued, these precipitates increased, indicating more extensive mineralization (**Figures 2, 3, and 4**).

At all time points, the chemical elemental composition of each experiment was evaluated using SEM/EDX. The full area was analyzed using EDX spectroscopy and included an area at

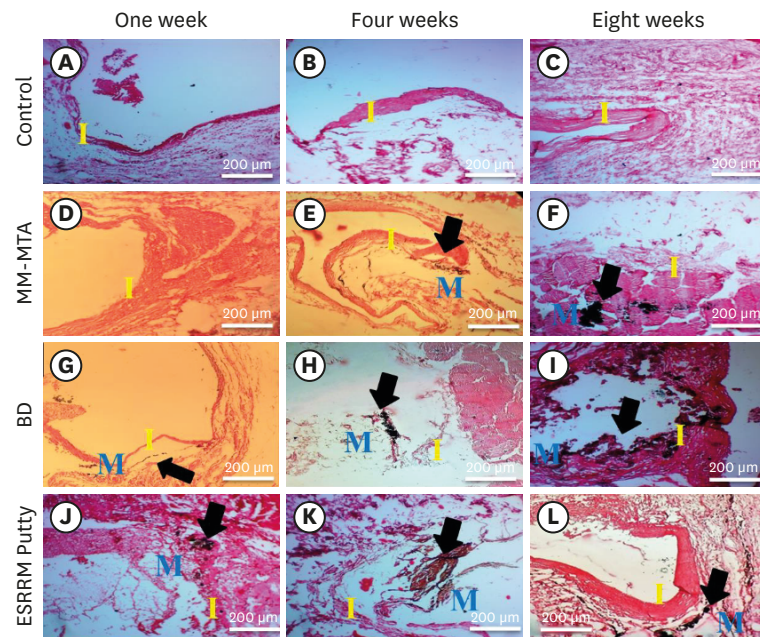


**Figure 1.** Histologic tissue sections demonstrating the biom mineralization (calcium deposition) in the experimental groups at the open ends of the subcutaneously-implanted silicon tubes at the 3 time points (weeks 1, 4, and 8). (A-C) Empty tubes: no dystrophic calcification was seen at any time point ( $\times 10$ ). (D) MM-MTA containing tubes: no calcification were seen at week 1 ( $\times 10$ ). (E and F) Black dystrophic calcifications were seen at weeks 4 and 8 (arrows,  $\times 10$ ). (G) BD-containing tubes: discrete deposits were seen at week 1 (arrow,  $\times 10$ ), and (H and I) more obvious dystrophic calcifications were seen at weeks 4 and 8 (arrows,  $\times 10$ ). (J-L) ESRRM putty-containing tubes: noticeable black dystrophic calcifications were obvious at all periods (arrows,  $\times 10$ ) (von Kossa stain, scale bar = 200  $\mu\text{m}$ ). MM-MTA, MicroMega mineral trioxide aggregate; BD, Biodentine; ESRRM, EndoSequence Root Repair Material; M, material; I, interface.

the material-tissue interface at which the concentrations of calcium and phosphorus were higher than those seen in the surrounding connective tissue (Figures 2, 3, and 4).

The EDX results showed that calcium and phosphorus concentrations in the 3 tested cements had increased over time with no statistically significant differences between cements, as shown in Table 2. According to these results, the calcium concentration found on the ESRRM putty was slightly greater than in the other groups at all time points.

The atomic ratio of calcium ions to phosphate ions (the calcium-to-phosphorus ratio) ranged from 2.4 to 4.27. No statistically significant differences in the calcium-to-phosphorus ratio were observed among the MM-MTA, BD, and ESRRM putty at all time points (Table 2).

## DISCUSSION

The capacity of a biomaterial to interact with living tissue allows the incorporation of the material into the environment and the expression of bioactivity. After implantation of bioactive materials, a series of biochemical and biophysical reactions occur at the material-tissue interface, resulting in biom mineralization [20]. Various approaches have recently been utilized to distinguish biom mineralization in intact tissues and cell cultures; staining with von Kossa stain, electron microscopic analysis, X-ray diffraction, and Fourier transform infrared spectroscopy are among the most common [21].

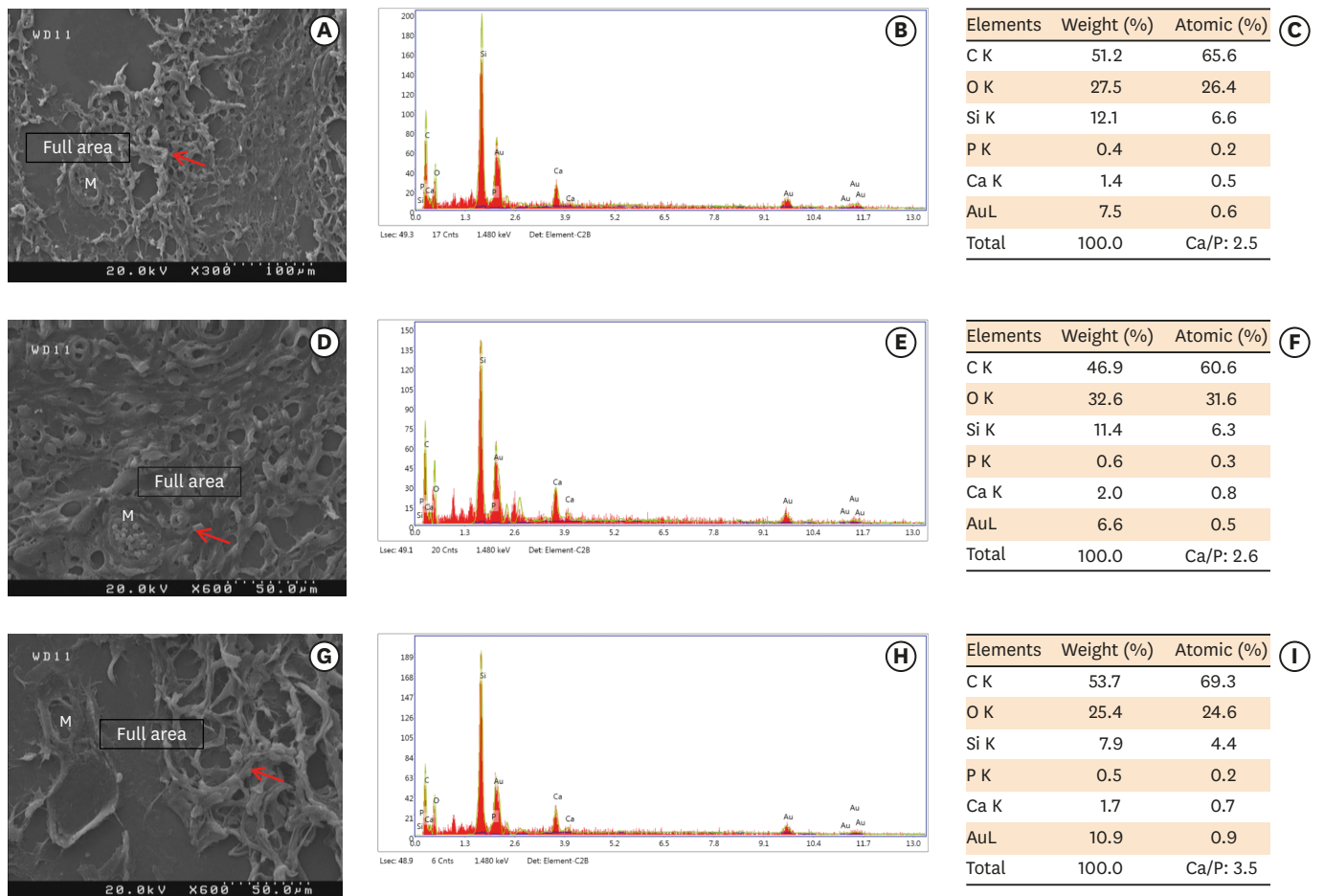


**Figure 2.** Scanning electron microscopy observations and elemental composition obtained using energy-dispersive X-ray analysis of the surface precipitates produced by (A-C) MM-MTA, (D-F) BD, and (G-I) ESRRM putty at 7 days after the subcutaneous implantation of the materials. Mineralization is indicated by the red arrows.

MM-MTA, MicroMega mineral trioxide aggregate; BD, Biodentine; ESRRM, EndoSequence Root Repair Material; M, material.

Assessments of the biom mineralization of different bioactive materials implanted in the subcutaneous tissue of a rat animal model using the von Kossa technique have been described previously [3,17,22-24]. This method is used for illustrating deposits of calcium or calcium salts. The principle behind staining is a precipitation reaction in which silver cations react with phosphate and carbonates in calcium deposits in the presence of acidic material. Photochemical degradation of silver phosphate to silver (visualized as black and metallic) then occurs under strong light illumination [25,26]. Furthermore, SEM and EDX analyses were used to gain a broader picture of the material's microstructure, chemistry, and compositional analyses. The calcium phosphate precipitation process, as well as the form and structure of the generated crystals, indicates the degree of bioactivity. The aim of this study was to assess biom mineralization using von Kossa stain and SEM/EDX analysis for material characterization after the implantation of silicon tubes filled with MM-MTA, BD, and ESRRM putty into rat subcutaneous tissue.

In the present study, all 3 tested calcium silicate-based cements exhibited positive von Kossa staining that increased over time. Additionally, all of the cements produced surface precipitates containing calcium and phosphorus after implantation into the dorsal surface

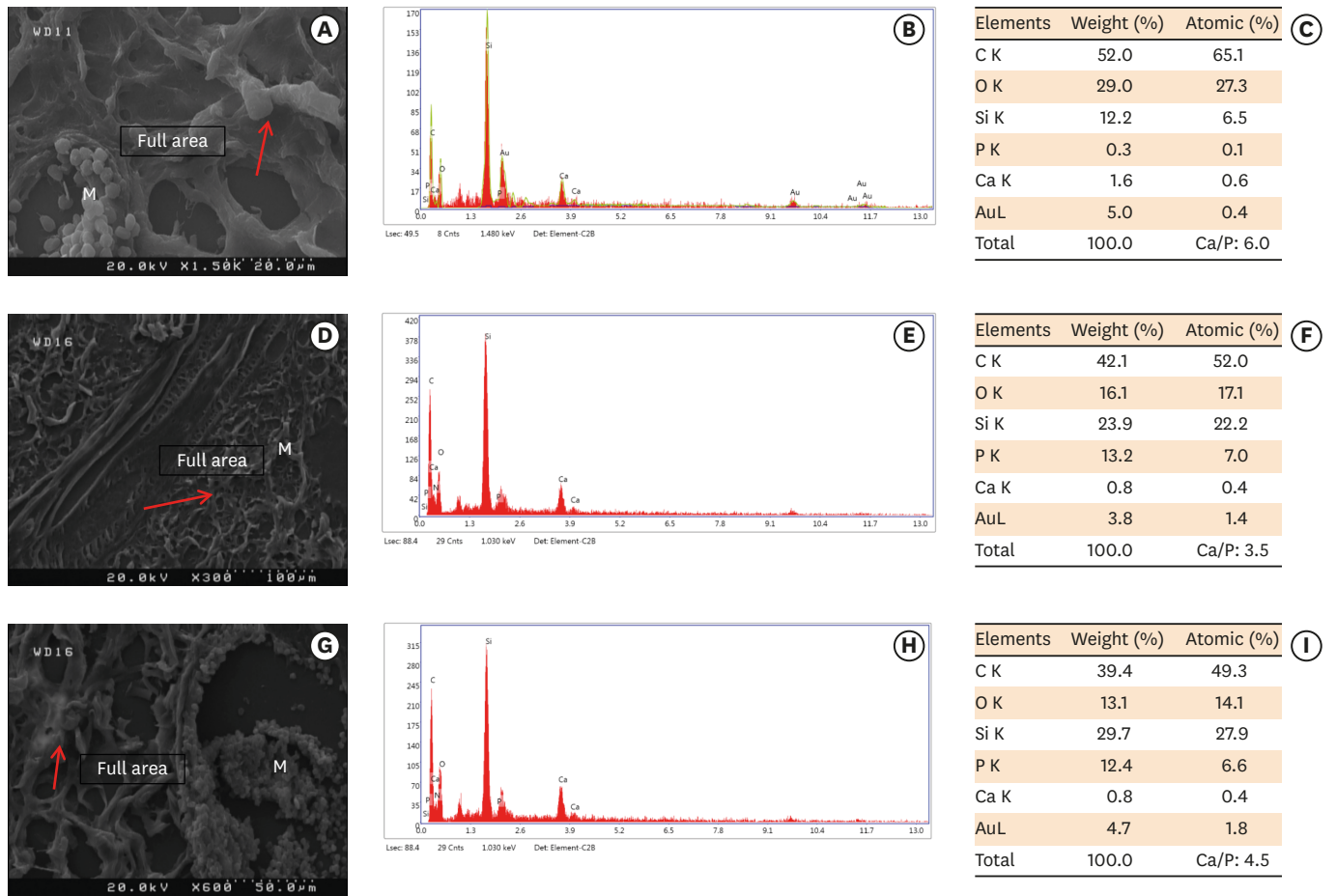


**Figure 3.** Scanning electron microscopy observations and elemental composition obtained using energy-dispersive X-ray analysis of the surface precipitates produced by (A-C) MM-MTA, (D-F) BD, and (G-I) ESRRM putty at 4 weeks after the subcutaneous implantation of the materials. Mineralization is indicated by the red arrows. MTA, MicroMega mineral trioxide aggregate; BD, Biodentine; ESRRM, EndoSequence Root Repair Material; M, material.

of rat subcutaneous connective tissue. This finding aligns with previous laboratory findings [17,18,27-29] and suggests that these materials are bioactive. The precipitates were most likely produced via the interaction of the calcium ions released from the materials with phosphate ions in body fluids, resulting in the formation of calcium phosphate crystalline structures on the materials' interfacial surfaces. In this study, calcium- and phosphorus-rich areas (which denoted biomineralization) were identified along the implant-tissue interface in all experiments. Moreover, these results indicate that the 3 tested cements were bioactive and caused biomineralization *in vivo*, although the degree and timing of biomineralization activity seemed to vary among the cements. In line with previously published literature [30,31], in the present study, the empty silicon tube produced no dystrophic calcification during any of the time periods.

Concerning root repair materials, the findings of this study support the ability of MM-MTA to induce biomineralization after implantation in the connective tissue due to the production of calcium and phosphorus surface precipitates at the interface between the tissue and the material [32]. The atomic calcium-to-phosphorus ratios in the MM-MTA cement samples at weeks 1, 4, and 8 were 2.5, 4.4, and 4.3, respectively. The lower ratio indicates an incomplete setting reaction and formation of stoichiometric hydroxyapatite during the first weeks, and the higher ratios after 4 and 8 weeks suggest calcium precipitation on the material's surface.

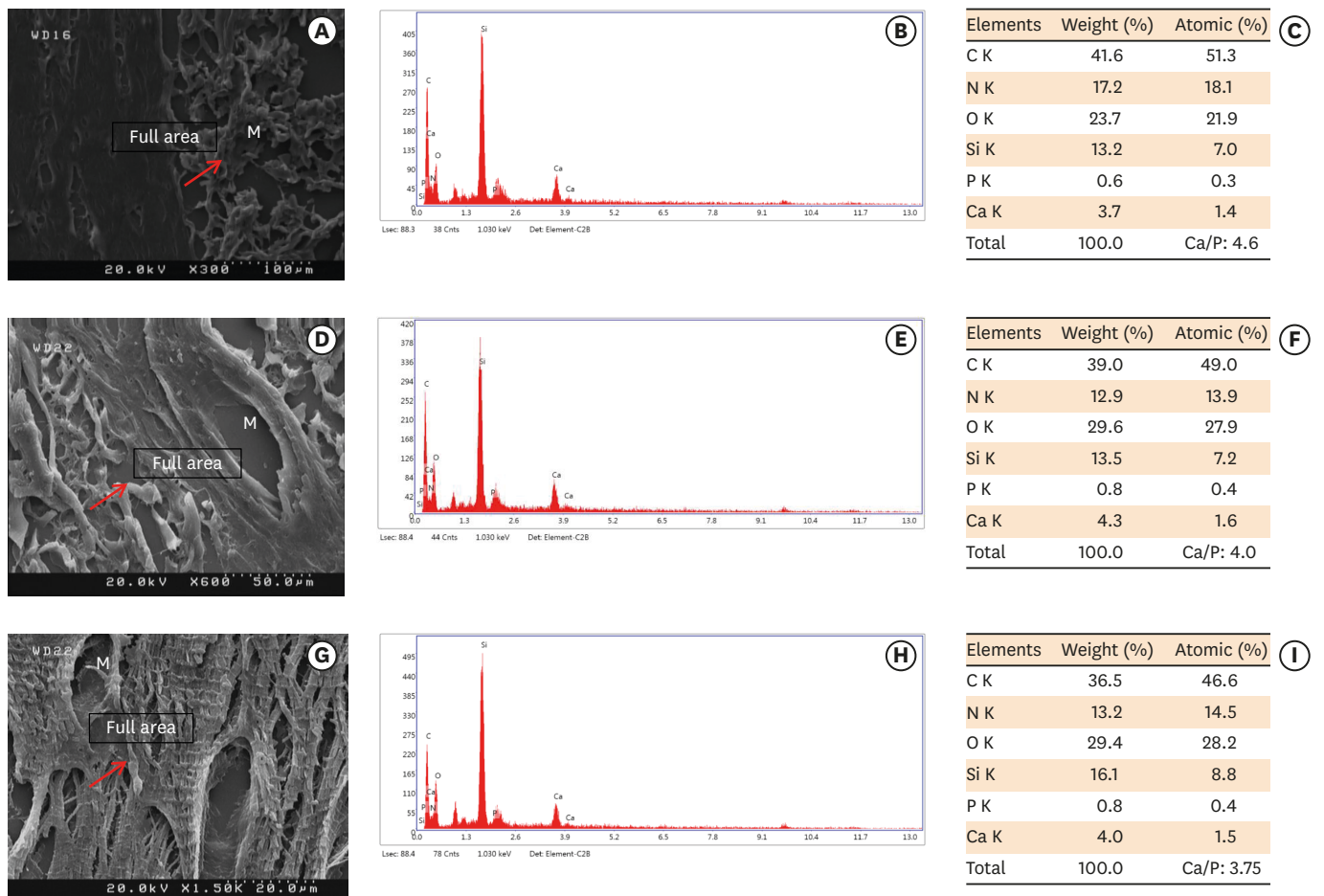


**Figure 4.** Scanning electron microscopy observations and elemental composition obtained using energy-dispersive X-ray analysis of the surface precipitates produced by (A-C) MM-MTA, (D-F) BD, and (G-I) EndoSequence Root Repair Material putty at 8 weeks after the subcutaneous implantation of the materials. Mineralization is indicated by the red arrows. MTA, MicroMega mineral trioxide aggregate; BD, Biodentine; ESRRM, EndoSequence Root Repair Material; M, material.

**Table 2.** Comparative semi-quantitative analysis of calcium- and phosphorus-rich areas of the 3 calcium silicate-based cements at 3 different time periods

Period	MM-MTA (atomic concentrations, %)			BD (atomic concentrations, %)			ESRRM putty (atomic concentrations, %)			p value
	Ca	P	Ca/P	Ca	P	Ca/P	Ca	P	Ca/P	
Week 1	0.5 ± 0.00	0.2 ± 0.00	2.5	0.633 ± 0.1527	0.266 ± 0.0577	2.4	0.667 ± 0.0577	0.3 ± 0.1732	2.63	> 0.05
Week 4	1.2333 ± 0.551	0.2667 ± 0.0577	4.433	1.1333 ± 0.4618	0.4667 ± 0.11547	3.433	1.75 ± 0.2516	0.425 ± 0.0957	4.32	> 0.05
Week 8	1.9 ± 0.707	0.45 ± 0.2121	4.3	2.2 ± 0.8485	0.5 ± 0.14142	4.3	2.2 ± 0.98995	0.5 ± 0.1414	4.27	> 0.05

Values are expressed as mean ± standard deviation.

Ca, calcium; P, phosphorus; MM-MTA, MicroMega mineral trioxide aggregate; BD, Biodentine; ESRRM, EndoSequence Root Repair Material.

However, positive von Kossa and dystrophic calcium particles were seen only in the relatively late period starting at 4 weeks after implantation. This result agrees with the findings of Yang *et al.* [23], who stated that von Kossa staining showed just a few calcified materials in the MTA group at week 8. Other published studies also indicated that MTA induced mineralization and granulations birefringent to polarized light in the subcutaneous tissues of rats after 30 days [17,19,33].

In an *in vitro* pulpo-dental animal model, the pulp-MTA interface showed growth of crystalline deposits [34] and dentinal bridges [35]. In extracted teeth (stored in synthetic fluid) and dentin disk (immersed in phosphate-buffered saline) models, MTA triggered the



initial precipitation of amorphous calcium phosphates, and the spontaneous precipitation then induced biom mineralization that led to the generation of an interfacial layer by 2 months into the experiments [7,36].

Several studies have reported the mineralization process of MTA. MTA is a strong alkaline substance, with a pH of approximately 12.5. It releases hydroxyl ions into adjacent tissues early in mineralization. This alkalinity stimulates mineralization through calcium ions that activate calcium-dependent adenosine triphosphatase [23,37]. The calcium ions also result in cell migration and differentiation [38]. Mineralization begins by forming calcium carbonate crystals as a nucleus of calcification when the calcium ions react with the carbon dioxide from the surrounding tissue [18]. In tissue culture and cutaneous tissue, the initiation and formation of a hard tissue require rich extracellular fibronectin [38], which forms the deposit within collagen fibrils of dentin in a tooth model [7]. This may explain the reasons for the induction of MTA later in implantation [7,36].

According to the present study, BD produced earlier calcification and was associated with more black deposits than MM-MTA at the end of the study. Calcification in the BD group started in week 1 and continued through weeks 4 and 8. This finding agrees with a study performed by Camilleri *et al.* [39] that indicated that the greater specific surface area and presence of calcium carbonate and calcium chloride in the composition of BD produced a greater rate of reaction than MTA. BD (unlike MTA, which is composed mainly of tricalcium silicate) is bioactive and can be hydrated into calcium silicate hydrate and calcium hydroxide (Portlandite), which reacts in the presence of physiological fluids to produce hydroxyapatite, mostly at the surface of the tricalcium silicate paste [40]. MTA, meanwhile, has a slower reaction rate and more porous microstructure; this is because it becomes hydrated more slowly than BD, as it contains a smaller amount of tricalcium silicate. However, it contains more calcium hydroxide byproduct than BD, resulting from the hydration of calcium oxide. This calcium hydroxide becomes hydrated very rapidly and induces an intense exothermic reaction [39]. Additionally, Gandolfi *et al.* [6] stated that BD released significantly more calcium ions than ProRoot MTA and MTA Angelus at 3 hours and at 1, 3, 7, 14, and 28 days, and this finding could relate to the presence of pure tricalcium silicate, calcium chloride, increased calcium hydroxide formation, and high solubility.

Furthermore, Setbon *et al.* [41] showed that the elemental composition of BD, as studied via inductively coupled plasma-atomic emission spectroscopy and EDX analysis, revealed the presence of 3 major components: oxygen, calcium, and silicon. The latter 2, which are important elements in the context of the interactions with pulp and periapical tissues and specifically regarding the formation of mineralized tissues (dentin and bone), presented in larger quantities than MM-MTA, which aligns with the previously cited works. Calcium and silicon are necessary for regulating the expression of genes that encode proteins such as bone morphogenetic protein 2 and osteopontin; additionally, they inhibit osteoclast activity and activate osteoblasts, thus inducing the creation of new bone and mineralization [42,43].

Despite these findings, an *in vivo* subcutaneous tissue model evaluation of the capacity of premixed ready-to-use fast-setting calcium silicate-based cement ESRRM putty to induce mineralization and promote calcification has not yet been conducted.

The histologic findings of the present study confirm that ESRRM putty has the property of inducing biom mineralization. Both Shokouhinejad *et al.* [44] and Ma *et al.* [45] reported the

induction of a hydroxyapatite or apatite-like layer on the ESRRM surface when it comes into contact with phosphate-containing fluids. This hard-tissue deposition is mainly attributed to the alkalinity of (with a pH greater than 12) and calcium ion release from ESRRM putty [46]. Based on our results, ESRRM putty, like BD and unlike MTA, showed the ability to induce calcification at an early time point. The stronger apatite-forming capability of ESRRM putty compared to MM-MTA may be attributed to the differences in their components, particle sizes, and bioactivity. Our result was consistent with findings by Hansen *et al.* [47], who concluded that diffusion of ions through root dentin was achieved at a shorter duration for ESRRM putty than for white MTA.

In the current study, the increasing calcium-to-phosphorus ratios acquired from conducting the EDX analyses on the BD, MM-MTA, and ESRRM putty cements at weeks 1, 4, and 8 suggest the incorporation of calcium into the cement, which indicates the existence of biocompatibility, bioactivity, and osteoconductivity.

Overall, this study is novel in that it involved simultaneous comparison of the timing of the biomineralization abilities of BD, MM-MTA, and ESRRM putty in the connective tissue of an animal model. It is recommended that further investigations using different techniques be performed *in vivo* and *in vitro* models, evaluating the timing and amount of dystrophic deposition in all 3 tested calcium silicate-based cements.

## CONCLUSIONS

Within the limitations of this study, we conclude that both the von Kossa-positive area and the calcium-to-phosphorus ratio of MM-MTA, BD, and EndoSequence Root Repair Material putty increased with time, indicating biomineralization activity after implantation in a rat subcutaneous model.

## ACKNOWLEDGEMENTS

The authors are indebted to Mrs. Ghodsie Morsali for her kind help and technical assistance.

## REFERENCES

1. Wang Z. Bioceramic materials in endodontics. *Endod Topics* 2015;32:3-30.  
[CROSSREF](#)
2. Koch KA, Brave DG. Bioceramics, part I: the clinician's viewpoint. *Dent Today* 2012;31:130-135.  
[PUBMED](#)
3. Bueno CR, Valentim D, Marques VA, Gomes-Filho JE, Cintra LT, Jacinto RC, Dezan-Junior E. Biocompatibility and biomineralization assessment of bioceramic-, epoxy-, and calcium hydroxide-based sealers. *Braz Oral Res* 2016;30:S1806-83242016000100267.  
[PUBMED](#) | [CROSSREF](#)
4. Jitaru S, Hodisan I, Timis L, Lucian A, Bud M. The use of bioceramics in endodontics - literature review. *Clujul Med* 2016;89:470-473.  
[PUBMED](#) | [CROSSREF](#)
5. Prati C, Gandolfi MG. Calcium silicate bioactive cements: biological perspectives and clinical applications. *Dent Mater* 2015;31:351-370.  
[PUBMED](#) | [CROSSREF](#)

6. Gandolfi MG, Siboni F, Botero T, Bossù M, Riccitiello F, Prati C. Calcium silicate and calcium hydroxide materials for pulp capping: biointeractivity, porosity, solubility and bioactivity of current formulations. *J Appl Biomater Funct Mater* 2015;13:43-60.  
[PUBMED](#) | [CROSSREF](#)
7. Reyes-Carmona JF, Felipe MS, Felipe WT. Biom mineralization ability and interaction of mineral trioxide aggregate and white Portland cement with dentin in a phosphate-containing fluid. *J Endod* 2009;35:731-736.  
[PUBMED](#) | [CROSSREF](#)
8. Torabinejad M, Parirokh M, Dummer PM. Mineral trioxide aggregate and other bioactive endodontic cements: an updated overview - part II: other clinical applications and complications. *Int Endod J* 2018;51:284-317.  
[PUBMED](#) | [CROSSREF](#)
9. Köseoğlu S, Pekbağr Yan K T, Kucukyilmaz E, Sağlam M, Enhos S, Akgün A. Biological response of commercially available different tricalcium silicate-based cements and pozzolan cement. *Microsc Res Tech* 2017;80:994-999.  
[PUBMED](#) | [CROSSREF](#)
10. Raghavendra SS, Jadhav GR, Gathani KM, Kotadia P. Bioceramics in endodontics - a review. *J Istanbul Univ Fac Dent* 2017;51(Supplement 1):S128-S137.  
[PUBMED](#) | [CROSSREF](#)
11. Köseoğlu S, Pekbağr Yan K T, Kucukyilmaz E, Sağlam M, Enhos S, Akgün A. Biological response of commercially available different tricalcium silicate-based cements and pozzolan cement. *Microsc Res Tech* 2017;80:994-999.  
[PUBMED](#) | [CROSSREF](#)
12. Escobar-García DM, Aguirre-López E, Méndez-González V, Pozos-Guillén A. Cytotoxicity and initial biocompatibility of endodontic biomaterials (MTA and Biodentine) used as root-end filling materials. *BioMed Res Int* 2016;2016:7926961.  
[PUBMED](#) | [CROSSREF](#)
13. Han L, Okiji T. Uptake of calcium and silicon released from calcium silicate-based endodontic materials into root canal dentine. *Int Endod J* 2011;44:1081-1087.  
[PUBMED](#) | [CROSSREF](#)
14. Atmeh AR, Chong EZ, Richard G, Festy F, Watson TF. Dentin-cement interfacial interaction: calcium silicates and polyalkenoates. *J Dent Res* 2012;91:454-459.  
[PUBMED](#) | [CROSSREF](#)
15. Charland T, Hartwell GR, Hirschberg C, Patel R. An evaluation of setting time of mineral trioxide aggregate and EndoSequence Root Repair Material in the presence of human blood and minimal essential media. *J Endod* 2013;39:1071-1072.  
[PUBMED](#) | [CROSSREF](#)
16. Tran D, He J, Glickman GN, Woodmansey KF. Comparative analysis of calcium silicate-based root filling materials using an open apex model. *J Endod* 2016;42:654-658.  
[PUBMED](#) | [CROSSREF](#)
17. Gomes Filho JE, Queiroz ÍO, Watanabe S, Cintra LT, Ervolino E. Influence of diabetes mellitus on the mineralization ability of two endodontic materials. *Braz Oral Res* 2016;30:S1806-83242016000100218.  
[PUBMED](#) | [CROSSREF](#)
18. Holland R, de Souza V, Nery MJ, Otoboni Filho JA, Bernabé PF, Dezan Júnior E. Reaction of rat connective tissue to implanted dentin tubes filled with mineral trioxide aggregate or calcium hydroxide. *J Endod* 1999;25:161-166.  
[PUBMED](#) | [CROSSREF](#)
19. Cintra LT, Ribeiro TA, Gomes-Filho JE, Bernabé PF, Watanabe S, Facundo AC, Samuel RO, Dezan-Junior E. Biocompatibility and biom mineralization assessment of a new root canal sealer and root-end filling material. *Dent Traumatol* 2013;29:145-150.  
[PUBMED](#) | [CROSSREF](#)
20. Hench LL. Bioceramics: from concept to clinic. *J Am Ceram* 1991;74:1487-1510.  
[CROSSREF](#)
21. Bonewald LF, Harris SE, Rosser J, Dallas MR, Dallas SL, Camacho NP, Boyan B, Boskey A. von Kossa staining alone is not sufficient to confirm that mineralization in vitro represents bone formation. *Calcif Tissue Int* 2003;72:537-547.  
[PUBMED](#) | [CROSSREF](#)
22. Camilleri J. Characterization of hydration products of mineral trioxide aggregate. *Int Endod J* 2008;41:408-417.  
[PUBMED](#) | [CROSSREF](#)

23. Yang WK, Ko HJ, Kim MR. Evaluation of the rat tissue reaction to experimental new resin cement and mineral trioxide aggregate cement. *Restor Dent Endod* 2012;37:194-200.  
[PUBMED](#) | [CROSSREF](#)
24. Bósio CC, Felipe GS, Bortoluzzi EA, Felipe MC, Felipe WT, Rivero ER. Subcutaneous connective tissue reactions to iRoot SP, mineral trioxide aggregate (MTA) Fillapex, DiaRoot BioAggregate and MTA. *Int Endod J* 2014;47:667-674.  
[PUBMED](#) | [CROSSREF](#)
25. Clark G. Staining procedures. Baltimore, MD: Williams and Wilkins; 1981. p187.
26. Gerstenfeld LC, Chipman SD, Glowacki J, Lian JB. Expression of differentiated function by mineralizing cultures of chicken osteoblasts. *Dev Biol* 1987;122:49-60.  
[PUBMED](#) | [CROSSREF](#)
27. Cosme-Silva L, Dal-Fabbro R, Gonçalves LO, Prado AS, Piazza FA, Viola NV, Cintra LT, Gomes Filho JE. Hypertension affects the biocompatibility and biom mineralization of MTA, High-plasticity MTA, and Biodentine®. *Braz Oral Res* 2019;33:e060.  
[PUBMED](#) | [CROSSREF](#)
28. Han L, Okiji T. Bioactivity evaluation of three calcium silicate-based endodontic materials. *Int Endod J* 2013;46:808-814.  
[PUBMED](#) | [CROSSREF](#)
29. Hinata G, Yoshiba K, Han L, Edanami N, Yoshiba N, Okiji T. Bioactivity and biom mineralization ability of calcium silicate-based pulp-capping materials after subcutaneous implantation. *Int Endod J* 2017;50(Supplement 2):e40-e51.  
[PUBMED](#) | [CROSSREF](#)
30. Yaltirik M, Ozbas H, Bilgic B, Issever H. Reactions of connective tissue to mineral trioxide aggregate and amalgam. *J Endod* 2004;30:95-99.  
[PUBMED](#) | [CROSSREF](#)
31. Ozbas H, Yaltirik M, Bilgic B, Issever H. Reactions of connective tissue to compomers, composite and amalgam root-end filling materials. *Int Endod J* 2003;36:281-287.  
[PUBMED](#) | [CROSSREF](#)
32. Bueno CR, Vasques AM, Cury MT, Sivieri-Araújo G, Jacinto RC, Gomes-Filho JE, Cintra LT, Dezan-Júnior E. Biocompatibility and biom mineralization assessment of mineral trioxide aggregate flow. *Clin Oral Investig* 2019;23:169-177.  
[PUBMED](#) | [CROSSREF](#)
33. Cintra LT, Benetti F, de Azevedo Queiroz ÍO, de Araújo Lopes JM, Penha de Oliveira SH, Sivieri Araújo G, Gomes-Filho JE. Cytotoxicity, biocompatibility, and biom mineralization of the new high-plasticity MTA material. *J Endod* 2017;43:774-778.  
[PUBMED](#) | [CROSSREF](#)
34. Tziafas D, Pantelidou O, Alvanou A, Belibasakis G, Papadimitriou S. The dentinogenic effect of mineral trioxide aggregate (MTA) in short-term capping experiments. *Int Endod J* 2002;35:245-254.  
[PUBMED](#) | [CROSSREF](#)
35. Dominguez MS, Witherspoon DE, Gutmann JL, Opperman LA. Histological and scanning electron microscopy assessment of various vital pulp-therapy materials. *J Endod* 2003;29:324-333.  
[PUBMED](#) | [CROSSREF](#)
36. Sarkar NK, Caicedo R, Ritwik P, Moiseyeva R, Kawashima I. Physicochemical basis of the biologic properties of mineral trioxide aggregate. *J Endod* 2005;31:97-100.  
[PUBMED](#) | [CROSSREF](#)
37. Seux D, Couble ML, Hartmann DJ, Gauthier JP, Magloire H. Odontoblast-like cytodifferentiation of human dental pulp cells in vitro in the presence of a calcium hydroxide-containing cement. *Arch Oral Biol* 1991;36:117-128.  
[PUBMED](#) | [CROSSREF](#)
38. Schröder U. Effects of calcium hydroxide-containing pulp-capping agents on pulp cell migration, proliferation, and differentiation. *J Dent Res* 1985;64:541-548.  
[PUBMED](#) | [CROSSREF](#)
39. Camilleri J, Sorrentino F, Damidot D. Investigation of the hydration and bioactivity of radiopacified tricalcium silicate cement, Biodentine and MTA Angelus. *Dent Mater* 2013;29:580-593.  
[PUBMED](#) | [CROSSREF](#)
40. Camilleri J. Characterization and hydration kinetics of tricalcium silicate cement for use as a dental biomaterial. *Dent Mater* 2011;27:836-844.  
[PUBMED](#) | [CROSSREF](#)

41. Setbon HM, Devaux J, Iserentant A, Leloup G, Leprince JG. Influence of composition on setting kinetics of new injectable and/or fast setting tricalcium silicate cements. *Dent Mater* 2014;30:1291-1303.  
[PUBMED](#) | [CROSSREF](#)
42. Murphy S, Wren AW, Towler MR, Boyd D. The effect of ionic dissolution products of Ca-Sr-Na-Zn-Si bioactive glass on in vitro cytocompatibility. *J Mater Sci Mater Med* 2010;21:2827-2834.  
[PUBMED](#) | [CROSSREF](#)
43. Kim EJ, Bu SY, Sung MK, Choi MK. Effects of silicon on osteoblast activity and bone mineralization of MC3T3-E1 cells. *Biol Trace Elem Res* 2013;152:105-112.  
[PUBMED](#) | [CROSSREF](#)
44. Shokouhinejad N, Nekoofar MH, Razmi H, Sajadi S, Davies TE, Saghiri MA, Gorjestani H, Dummer PM. Bioactivity of EndoSequence root repair material and bioaggregate. *Int Endod J* 2012;45:1127-1134.  
[PUBMED](#) | [CROSSREF](#)
45. Ma J, Shen Y, Stojicic S, Haapasalo M. Biocompatibility of two novel root repair materials. *J Endod* 2011;37:793-798.  
[PUBMED](#) | [CROSSREF](#)
46. Dawood AE, Parashos P, Wong RH, Reynolds EC, Manton DJ. Calcium silicate-based cements: composition, properties, and clinical applications. *J Investig Clin Dent* 2017;8:e12195.  
[PUBMED](#) | [CROSSREF](#)
47. Hansen SW, Marshall JG, Sedgley CM. Comparison of intracanal EndoSequence Root Repair Material and ProRoot MTA to induce pH changes in simulated root resorption defects over 4 weeks in matched pairs of human teeth. *J Endod* 2011;37:502-506.  
[PUBMED](#) | [CROSSREF](#)